

and  $|\mathcal{M}|^2$  is the Fermi matrix element. Recent  $ft$ -values<sup>4,6,7</sup> for the  $0 \rightarrow 0$  transition in  $O^{14}$ ,  $Al^{26}$ , and  $Cl^{34}$  give  $A = 6200 \pm 100$ . This value of  $A$  and recent  $ft$ -values<sup>4</sup> for the mirror transition in  $O^{15}$  and  $F^{17}$ , which are closed shells  $\pm$  one nucleon, give  $R = 1.17 \pm 0.10$ .

The resulting Gamow-Teller matrix element for  $K^{37}$  is  $0.38 \pm 0.08$ , which is in agreement with the theoretical

value 0.32 that Winther and Kofoed-Hansen have calculated from the shell model. The error in the experimental value of the Gamow-Teller matrix element is now principally due to the error in the end point of the  $K^{37}$  positron spectrum.

ACKNOWLEDGMENT

I am grateful to Professor J. R. Richardson for suggesting this problem and for his interest and guidance.

<sup>6</sup> Bromley, Almqvist, Gove, Litherland, Paul, and Ferguson, Phys. Rev. **105**, 957 (1957).

<sup>7</sup> D. Green and J. R. Richardson, Phys. Rev. **101**, 776 (1956).

Photoprotons from  $N^{15}\dagger$

JACOB L. RHODES\* AND W. E. STEPHENS  
 University of Pennsylvania, Philadelphia, Pennsylvania  
 (Received February 20, 1958)

The photoprotons ejected by bremsstrahlung photons from nitrogen gas enriched in  $N^{15}$  were detected in nuclear emulsions and the proton energy and angular distributions measured for 18.7- and 24.6-Mev betatron energies. The photoproton yield is  $10^6$  protons per atomic weight per roentgen unit at 24.6 Mev. The integrated cross section in the giant resonance is 10-Mev millibarns for ground-state transitions. Structure is observed in the giant resonance and the angular distributions in this region are predominantly  $\sin^2\theta$ .

INTRODUCTION

THE excitation of nuclei by high-energy photons is enhanced in the "giant resonance" region and can be detected by observing the ejected photoparticles. Such observations can give information concerning highly excited states of the absorbing nucleus. The high available intensity of bremsstrahlung radiation can be utilized in those cases where the resultant nucleus has wide spacing between levels, so that a measurement of photoproton energy identifies the absorbed photon energy. The reaction  $N^{15} + \gamma \rightarrow C^{14} + H^1 - 10.207$  Mev is especially favorable since the first excited state of  $C^{14}$  is at 6.091 Mev. Furthermore, the  $N^{15}$  ground state is  $\frac{1}{2}^-$ , different from isotopes previously examined here.<sup>1</sup> The

resolution attainable using nuclear emulsion recording of the photoprotons is about 0.2 Mev. We have therefore observed the photoprotons from  $N^{15}$ , using betatron bremsstrahlung and nuclear emulsion detectors.

EXPERIMENT

A well-collimated bremsstrahlung x-ray beam from the betatron passes through the reaction chamber shown in Fig. 1. This aluminum chamber contains the gas to be irradiated and the nuclear emulsion plates to detect the photoprotons. It is lined with  $\frac{1}{32}$ -inch lead to reduce the proton background. Details of the several runs are given in Table I. 200-micron Ilford C-2 nuclear emulsion plates were used and scanned with a Leitz Ortholux microscope at a magnification of 848. The proton ranges were corrected for absorption in the gas and for photon momentum, and the proton energies determined from Rotblat's range-energy data. Background was deter-

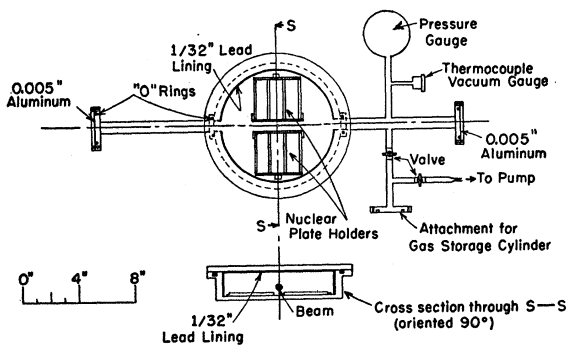


FIG. 1. The reaction chamber.

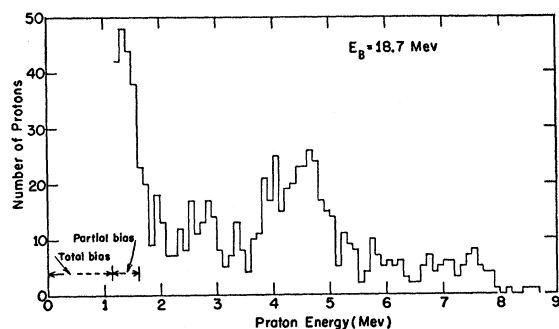


FIG. 2. Photoproton energy distribution for 18.7-Mev exposure.

<sup>†</sup> Supported in part by the joint program of the Office of Naval Research and the U. S. Atomic Energy Commission.

\* Now at Lebanon Valley College, Annville, Pennsylvania.

<sup>1</sup> Cohen, Mann, Patton, Reibel, Stephens, and Winhold, Phys. Rev. **104**, 108 (1956).

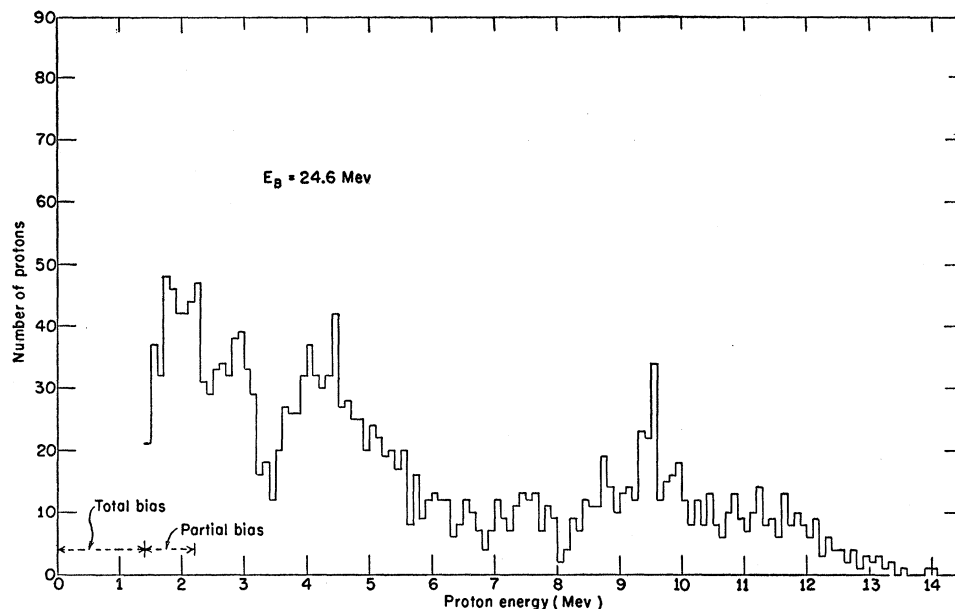


FIG. 3. Photoproton energy distribution for 24.6-Mev exposure.

mined from scanning runs *X*, *D*, and *Y*. It was estimated to be about  $\frac{3}{2}$  protons per energy interval from 2 to 8 Mev and  $\frac{1}{2}$  proton per interval above 8 Mev in the 24.6-Mev run. In the 18.7-Mev run, the background was estimated to be 1 proton per energy interval above 2 Mev. These background protons seem to be rather uniformly distributed in energy.

The energy resolution is estimated to be about 200 kev at 3- and 10-Mev proton energy, dipping to a minimum of 150 kev at 5-Mev proton energy. This is mainly due to straggling in the emulsion and gas plus an additional uncertainty due to width of the x-ray beam. The accuracy of proton energy is estimated to be about 100 kev.

### RESULTS

Figures 2 and 3 exhibit the energy distributions of the photoprotons for the 18.7-Mev and 24.6-Mev runs respectively. These histograms include all acceptable tracks observed in the angle range from  $30^\circ$  to  $150^\circ$  with respect to the photon beam direction. The proton energy region in which all the protons would be completely absorbed before making a recognizable track in the emulsion is indicated as "total bias." "Partial bias" designates the energy region in which some protons

were prevented by gas absorption from being recorded. Ejection of protons of less than 1 Mev should be inhibited by the Coulomb barrier.

When the proton distribution in Fig. 2 (18.7-Mev run) has been corrected for difference in bremsstrahlung photon distribution at 18.7 and 24.6 Mev and subtracted from Fig. 3 (24.6-Mev run), the difference represents the numbers of photoprotons emitted leaving the  $C^{14}$  nucleus in an excited state. This distribution is shown in Fig. 4. These protons cannot now be uniquely identified with the photon energy absorbed due to the multiplicity of possible  $C^{14}$  excited states. Nevertheless it can be noted that there are almost twice as many transitions to excited states as to the ground state after photon absorption in the 18- to 24-Mev range.

The angular distributions of the photoprotons have been determined for various energy groups and is tabulated in Table II and shown in Figs. 5, 6, 7, and 8. In the 18.7-Mev run, the protons are emitted in transi-

TABLE I. Details of exposures.

Run	Gas	Pressure (mm Hg)	Beta-tron energy (Mev)	Irradiation (roentgens)	Exposure time (days)	Area scanned (mm <sup>2</sup> )	Tracks measured
A	Nitrogen-15 (95.7%)	845	24.6	22 600	3	189	2183
B	Nitrogen-15 (95.7%)	845	18.7	18 700	4	105	912
X	Nitrogen-14	36.4	24.6	10 900	2	63	21
D	Nitrogen-14	855	24.6	20 400	3	21	396
Y	Nitrogen-14	36.4	18.7	9 870	2	63	13

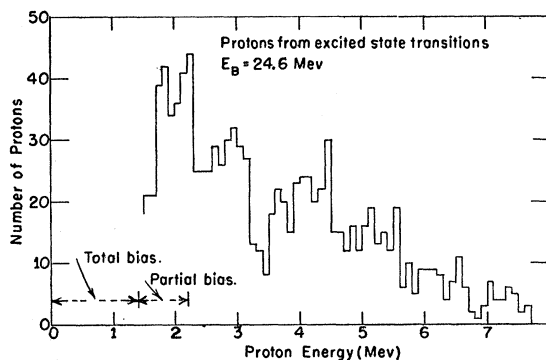


FIG. 4. Energy distribution of protons from excited-state transitions.

tions from the excited intermediate states of N<sup>15</sup> to the ground state of C<sup>14</sup>. In the 24.6-Mev run this is also true for all protons over 8 Mev.

The x-ray beam intensity was monitored by an ionization chamber calibrated against a Victoreen 100 r-meter in a 9.5-cm diameter Lucite cylinder. Using the Schiff spectrum as tabulated by Nathans,<sup>2</sup> corrected for absorption in the beam, and the r-meter response calculated by Zendle *et al.*<sup>3</sup> the observed photoproton yield can be transformed into cross section.

The average yield of N<sup>15</sup> photoprotons with 18.7-Mev bremsstrahlung was found to be  $2.17 \times 10^4$  protons per atomic weight per roentgen unit. The 24.6-Mev yield was  $1.12 \times 10^5$  protons (atomic wt)<sup>-1</sup> r<sup>-1</sup>. The yield of photoprotons from N<sup>14</sup> was found in run D to be

TABLE II. Observed angular distribution parameters.  
 $f(\theta) = A + B \sin^2\theta(1 + \beta \cos\theta)^2$ .

Energy groups in Mev	A/B	$\beta$
18.7-Mev run		
2.2- 3.5	isotropic	
3.5- 5.6	$1.20 \pm 0.30$	
5.6- 8.0	$0.27 \pm 0.36$	
1.8- 8.0	$1.39 \pm 0.44$	0.26
24.6-Mev run		
2.4- 3.5	isotropic	
3.5- 5.6	$1.17 \pm 0.34$	
5.6- 8.0	$1.00 \pm 0.38$	
8.0- 9.3	$0.81 \pm 0.59$	
9.3- 9.6	$0.00 \pm 0.12$	
9.6-10.1	$0.16 \pm 0.25$	
10.1-14.0	$0.26 \pm 0.17$	
8.0-14.0	$0.25 \pm 0.18$	0.24

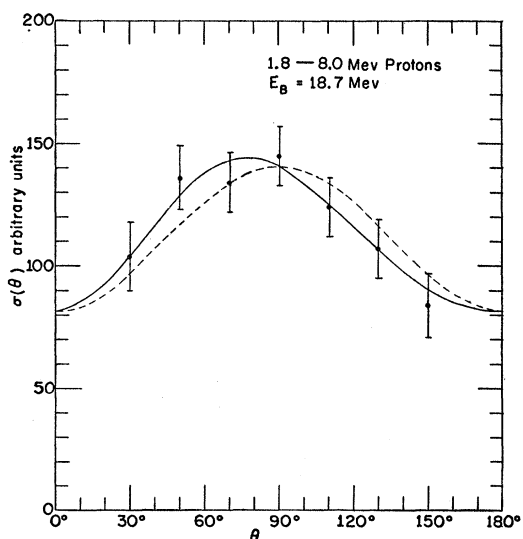


FIG. 5. Angular distribution of protons with 1.8- to 8.0-Mev energy in the 18.7-Mev run.

<sup>2</sup> R. Nathans, Ph.D. thesis, University of Pennsylvania, 1954 (unpublished).

<sup>3</sup> Zendle, Koch, McIlhinney, and Boag, Radiation Research 5, 107 (1956).

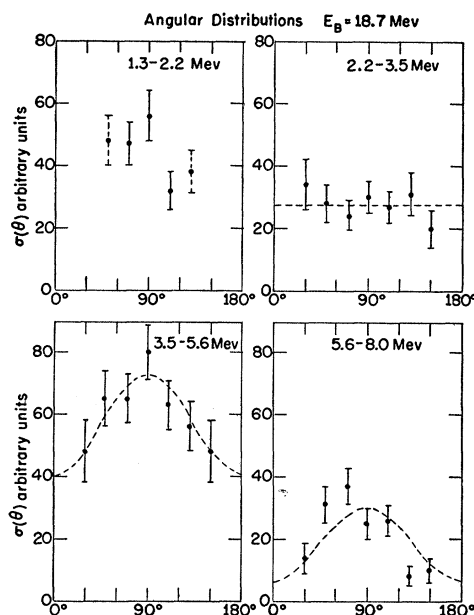


FIG. 6. Angular distributions from 18.7-Mev run for protons of energy: (a) 1.3 to 2.2 Mev, (b) 2.2 to 3.5 Mev, (c) 3.5 to 5.6 Mev, and (d) 5.6 to 8.0 Mev.

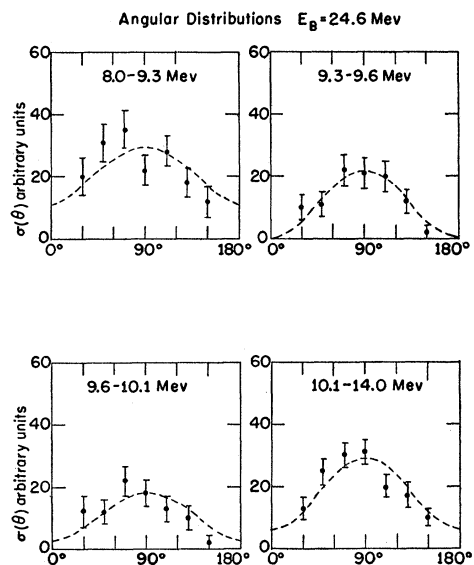


FIG. 7. Angular distributions from 24.6-Mev run for protons of energy: (a) 8.0 to 9.3 Mev, (b) 9.3 to 9.6 Mev, (c) 9.6 to 10.1 Mev, and (d) 10.1 to 14.0 Mev.

$(1.8 \pm 0.4) \times 10^5$  protons (atomic wt)<sup>-1</sup> r<sup>-1</sup>. The N<sup>15</sup> photoproton yields can be corrected for angular distribution to  $(2.06 \pm 0.2) \times 10^4$  protons (atomic wt)<sup>-1</sup> r<sup>-1</sup> at 18.7 Mev and  $(1.06 \pm 0.14) \times 10^5$  protons (atomic wt)<sup>-1</sup> r<sup>-1</sup> at 24.6 Mev.

The cross section for absorption of photons by N<sup>15</sup> leading to the emission of a proton leaving C<sup>14</sup> in its ground state can be deduced from Figs. 2 and 3 and the bremsstrahlung photon distributions. This cross

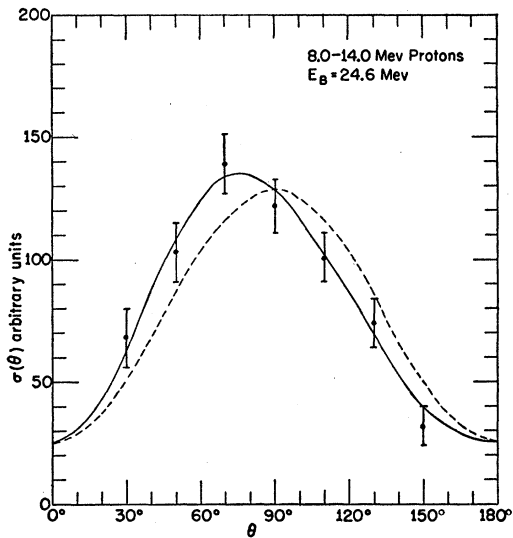


FIG. 8. Angular distribution of protons with 8.0- to 14.0-Mev energy in the 24.6-Mev run.

section is shown in Fig. 9 as a function of photon energy. Only the statistical uncertainties are shown by the vertical lines. An additional uncertainty of about 10% is imposed by the photon intensity calibration. The dotted curve in Fig. 9 is the cross section predicted from measurements on the inverse<sup>4</sup> reaction  $C^{14}(p,\gamma)N^{15}$  using detailed balancing, and is in good agreement with the photoproton cross section.

The integrated cross section for photoproton production can be estimated from such curves to be 3.9 Mev-mb up to 18.7 Mev, 14.5 Mev-mb for ground state transitions up to 24.6 Mev, and  $38 \pm 5$  Mev-mb total.

A few alpha particles were observed, indicating yields of 200 and 1200 alphas per atomic weight per roentgen at 18.7 and 24.6 Mev, respectively. With these yields in mind and the observations of Muller and Stoll<sup>5</sup> on photodeuterons and tritons from boron, we estimate the contribution to our results of photodeuterons and

tritons to be less than 3 Mev-mb, and because of energy considerations not to affect the ground-state transition cross-section curve.

#### DISCUSSION

The ground-state transition cross-section curve shown in Fig. 9 indicates several resonances which can be interpreted as levels in excited  $N^{15}$ . The large numbers of protons below 2.2 Mev in Fig. 2 are associated with excitation to an 11.6-Mev level in  $N^{15}$  and transition to the ground state in  $C^{14}$  giving a peak in the cross-section curve at 11.6 Mev. This level is known from the inverse reaction  $C^{14}(p,\gamma)N^{15}$  to be a  $\frac{1}{2}^+$  level with a width of 475 kev.<sup>4</sup> Consequently, this would correspond to row 1 in Table III and would require isotropic angular distribution of the emitted protons. Since these photoprotons are in the region of "partial bias" due to gas absorption, the observed angular distribution is incomplete but consistent with isotropy.

The next large group of protons in Fig. 2 is at 4.5 Mev corresponding to the peak at 15 Mev in Fig. 9. The angular distribution has a ratio  $A/B = 1.2 \pm 0.3$  which is consistent with electric or magnetic dipole absorption into a  $\frac{3}{2}^{\pm}$  level in  $N^{15}$ . This level (or group of levels) may correspond to the "pygmy resonance" found in other light nuclei, but here certainly it is not associated with electric quadrupole absorption. All the protons observed in the 18.7-Mev run are consistent with  $E1$  or  $M1$  absorption and very little quadrupole interference below 16 Mev. Above 16 Mev the isotropic component is somewhat less than would be expected from  $E1$  and  $M1$  absorption in isolated levels; however, the statistical errors in these angular distributions of the 18.7-Mev run are large.

The angular distribution of protons greater than 9 Mev in the 24.6-Mev run are predominantly  $\sin^2\theta$ . These protons correspond to the cross-section curve of Fig. 9 above 20 Mev, i.e., the giant resonance region. From Table III all the expected distributions for compound nucleus transitions from single levels should

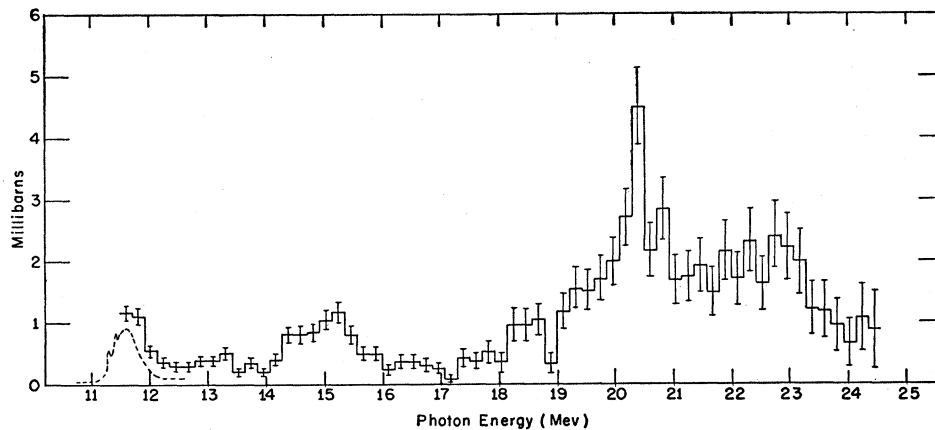


FIG. 9. Variation with energy of the cross section for ground-state transitions in  $N^{15}(\gamma,p)C^{14}$ . Dotted curve is derived from the inverse reaction  $C^{14}(p,\gamma)N^{15}$  by detailed balancing.

<sup>4</sup> Bartholomew, Brown, Gove, Litherland, and Paul, Can. J. Phys. 33, 441 (1955).

<sup>5</sup> R. Muller and P. Stoll, Helv. Phys. Acta 26, 207 (1953).

TABLE III. Calculated angular distributions (using *j-j* coupling) for various compound nuclear state transitions in N<sup>15</sup>( $\gamma, p$ )C<sup>14</sup>.

N <sup>15</sup> ground state <i>J<sub>i</sub></i>	C <sup>14</sup> state <i>J<sub>f</sub></i>	Type of photon absorption	N <sup>15</sup> excited state <i>J<sub>e</sub></i>	Emitted proton angular momentum <i>l<sub>p</sub></i>	Angular distribution of emitted proton <i>f</i> ( $\theta$ )	
$\frac{1}{2}^-$	0 <sup>+</sup> ground state or 6.894-Mev excited state	<i>E1</i>	$\frac{1}{2}^+$	0	isotropic	
			$\frac{3}{2}^+$	2	$2+3 \sin^2\theta$	
		<i>M1</i>	$\frac{1}{2}^-$	1	isotropic	
			$\frac{3}{2}^-$	1	$2+3 \sin^2\theta$	
			$\frac{5}{2}^-$	1	$1+\cos^2\theta$	
			$\frac{7}{2}^-$	3	$1+6 \cos^2\theta - 5 \cos^4\theta$	
		0 <sup>-</sup> possibly 6.589-Mev state <i>E1</i>	<i>E1</i>	$\frac{1}{2}^+$	1	isotropic
				$\frac{3}{2}^+$	1	$2+3 \sin^2\theta$
		1 <sup>-</sup> 6.091-Mev or possibly 6.589-Mev state	<i>E1</i>	$\frac{1}{2}^+$	1	isotropic
				$\frac{3}{2}^+$	1	$\begin{cases} 2+3 \sin^2\theta & (S=\frac{1}{2}) \\ 4+3 \sin^2\theta & (S=\frac{3}{2}) \end{cases}$
					3	$1+\sin^2\theta$
		2 <sup>-</sup> 6.723-Mev, 7.346-Mev, or possibly 6.589-Mev state	<i>E1</i>	$\frac{1}{2}^+$	1	isotropic
				3	isotropic	
			$\frac{3}{2}^+$	1	$\begin{cases} 4+3 \cos^2\theta & (S=\frac{3}{2}) \\ 6+\sin^2\theta & (S=\frac{5}{2}) \end{cases}$	
				3	$\begin{cases} 1+\sin^2\theta & (S=\frac{3}{2}) \\ 19+3 \cos^2\theta & (S=\frac{5}{2}) \end{cases}$	

have an  $A/B \geq 0.66$ ; actually  $A/B$  is observed to be less than 0.4. The angular distribution to be expected on the Wilkinson "resonance direct" picture from single-shell states is also  $A/B \geq 0.66$ . The alpha-particle model is not appropriate for ground-state transitions. Consequently the observed angular distribution requires a different explanation. Since both  $\frac{1}{2}^+$  and  $\frac{3}{2}^+$  states are accessible by electric dipole absorption in N<sup>15</sup>, and since such states may overlap (for example, the 11.61-Mev  $\frac{1}{2}^+$  state has a width of 475 kev and the 11.80-Mev

$\frac{3}{2}^+$  state is 38 kev wide),<sup>4</sup> the emitted proton waves can interfere and show angular distributions different from those of Table III. It seems that with appropriate mixing, the isotropic terms can cancel, leaving the  $\sin^2\theta$  distribution.

ACKNOWLEDGMENTS

We gratefully acknowledge helpful discussions with Professor K. Brueckner, Professor S. Frankel, Dr. E. G. Muirhead, and Dr. R. Amado.